Journal of Civil Engineering, Science and Technology
Volume 10, Issue 2, September 2019

IDENTIFICATION OF FLOODED AREAS DUE TO SEVERE STORM USING ENVISAT ASAR DATA AND NEURAL NETWORKS

A. Abhyankar[1*], A. Patwardhan[1], M. Paliwal[2] and A. Inamdar[3]
[1]National Institute of Construction Management and Research, Pune, India.
[2]Persistent Systems, Nagpur, India.
[3]Indian Institute of Technology Bombay, Mumbai, India.

Date received: 04/06/2019, Date accepted: 04/09/2019
*Corresponding author's email: aabhyankar@nicmar.ac.in
Doi: 10.33736/jcest.1531.2019

Abstract —The specific objective of the present study is to identify flooded areas due to cyclonic storm using Envisat ASAR VV polarized data and Artificial Neural Network (ANN). On October 30, 2006, the Ogni storm crossed the Indian coast. It impacted three coastal districts in Andhra Pradesh, including Guntur, Prakasam, and Krishna. The present study considers only nine mandals of Guntur district of Andhra Pradesh for identification of flooded areas. For this purpose, pre and post event images of study area were procured of Envisat satellite (April 23, 2006 and November 4, 2006). Field visit to the affected district after the disaster was carried out to gather landcover information. In all, 564 pixels landcover information was collected during the visit (These were corresponding to pre event Envisat image of April 23, 2006). Out of the 564 pixels, randomly 406 pixels (91 were water and the remaining 315 were non-water pixels) were used for training the Neural Network and the remaining for testing. Using the trained ANN model, the total water area in the nine mandals of Guntur using Envisat ASAR satellite imagery of April 23, 2006 was found to be 2.344 thousand hectares. The trained model was applied to the post event Envisat ASAR image of November 4, 2006 to obtain completely submerged and partial/non submerged areas under water. The completely submerged landcover under water in nine mandals of Guntur district on November 4, 2006 was found to be 13.2705 thousand hectares. Results suggest a high accuracy of classification and indicate that this may be a rapid tool for damage estimation and post disaster relief and recovery efforts.

Keywords: Envisat ASAR, Remote Sensing, Artificial Neural Network (ANN), floods

1.0 INTRODUCTION

The Indian subcontinent encounters a number of natural hazards namely, tropical cyclones, landslides, earthquakes, floods, heat waves, etc. The most frequent among them are cyclones. It was found that on average, around 8 or 9 cyclones of different intensities annually cross Indian coastline [1]. Tropical cyclones caused enormous damaged and had a socio-economic impact. The damages were caused by strong winds, storm surges, and heavy rainfalls. Cyclones caused loss of lives and properties, inundate coastal regions, especially with low-lying areas, erode embankments, beaches, and reduce the fertility of soil. Sources of drinking water were polluted by coastal inundation and resulting in the outbreak of epidemics.

Various satellites had been launched during the last three decades for observing the happenings on the earth. The satellites with optical sensors had been extensively used in natural resource management (e.g. Landsat, SPOT, Quickbird, Ikonos, IRS satellites, etc.) and national development applications. Application of satellites with optical sensors for monitoring gets reduced during and immediately after the floods/cyclone. This is due to the cloud cover during floods/cyclonic event. The availability of optical images after few days of the cyclonic event resulted in under estimation of submergence and damage results. Radar had inherent cloud penetration capability and distinctive water response. It was a valuable tool, which can be used to monitor floods. While monitoring floods, its availability during all weather conditions and under extreme atmospheric conditions, Synthetic Aperture Radar (SAR) was found to be very useful and was well documented in the literature [2; 3; 4; 5].

In the initial period itself, Seasat and Shuttle Imaging Radar (SIR) showed the SAR data applicability in monitoring floods [6]. Later during the past two decades, various SAR satellites were launched namely, Radarsat-1/2 [7; 8], Envisat ASAR [9; 10], JERS [11], ERS-1/2 [12] which were used in flood monitoring.

Water bodies had least backscattering values in microwave regions. Moreover, plain water and completely submerged landcovers under water had the same backscattering range [13; 14]. The observation revealed that flooded areas and open water would be identified easily with like-polarized (HH and VV) rather than cross-polarized (HV) data [15].

In the past, deterministic approach was used to classify water and non-water landcover classes using SAR [16]. Studies in the past had shown an overlap in the backscattering values of water and non-water landcovers. The deterministic threshold approach will lead to overestimation or underestimation of water areas and submerged area [17; 18]. This approach reduced the overall errors of estimation of water and flooded areas, but the assumption of normality continued to exist. To overcome this assumption, the present study attempts to identify water and flooded areas using Envisat ASAR VV band and a feed forward neural network. This is a non-threshold based non-parametric approach. This approach does not depend upon assumptions that there is an underlying distribution for backscattering values.

2.0 STUDY AREA

On October 30, 2006, the Ogni storm crossed the coast of Andhra Pradesh. The storm impacted the following coastal districts in Andhra Pradesh, Guntur, Prakasam, and Krishna. Figure 1 depicts the districts affected by Ogni storm. In Guntur district alone, nearly 15,000 houses were severely damaged, nearly one-lakh hectares of paddy got inundated, and 12 people died due to this event [19].

In the present study, a part of Guntur district was considered as study area. In all, nine mandals of the Guntur district were considered for damage assessment, namely Tenali, Tsunder, Vemuru, Amruthalur, Cherukupalle, Pittalavanipalem, Karlapalem, Nagaram and Nizampatnam as these areas were reportedly impacted by this storm. The total geographical area of the nine mandals was 111 thousand hectares [20; 21] and the map area using Geographic Information Systems (GIS) was found to be 116.35 thousand hectares.

The predominant landcover was paddy with a rural setting. The study area i.e. nine mandals considered for damage assessment of Guntur district due to this storm is given in Figure 2. A field visit to Guntur district of Andhra Pradesh was carried out after the cyclonic event. During the field visit, hand held Global Positioning System (GPS) was used to collect information of land cover classes.

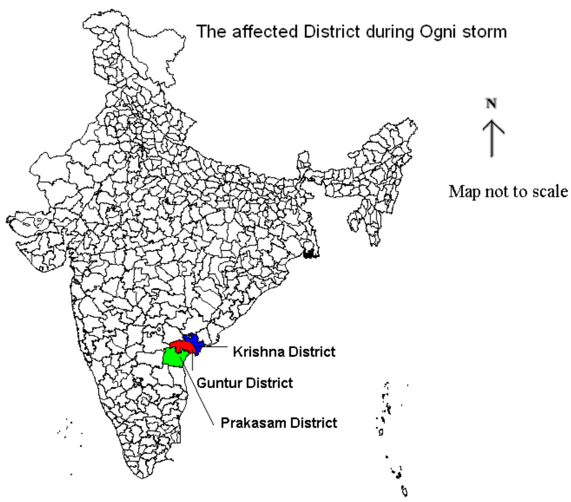

Figure 1 Affected districts during Ogni storm

Figure 2 Study area in the Guntur district considered for damage assessment due to Ogni storm

3.0 PREPROCESSING OF ENVISAT ASAR DATA

The pre and post event images of Envisat ASAR were obtained from European Space Agency (ESA). The pre event image of April 23, 2006 was acquired in IS4 (swath), descending mode with HH and VV polarization, whereas the post event image of Envisat ASAR of November 4, 2006 was acquired in IS4 (swath), ascending mode with VV and VH polarization. Both the scenes were obtained in the Single Look Complex (SLC) format.

To compare temporal data for performing a quantitative analysis, one requires absolute calibration. For DN to sigma-0 (backscattering coefficient) conversion, we developed software using the algorithms [22]. Other processing steps such as slant to ground range and geocoding were performed using ENVI software.

As described in ESA document, the backscattering coefficient ($\sigma°$) values were obtained by combining the radar pixel intensity and the incidence angle (I_j) at each pixel location, where the angle of incidence was obtained from the ASAR header data using interpolation method and is given in Equation 1.

$$\sigma\sigma_j° = \left(\frac{DN2}{K} \times \frac{R_d}{R_{ref}}\right).4 \times \left(\frac{1}{G2}\right) \times \sin I_j \qquad (1)$$

Where;
K is the absolute calibration constant,
DN2 is the pixel intensity,
G2 is two-way antenna gain at distributed target look angle,
Rd is distributed target slant range distance and Rref is reference slant range distance.

The relationships between incidence angle (αj), Earth angle (γj), slant range distance (R_j), satellite to Earth centre distance (R_{sat}) and elevation angle (θ_j) are given in Equation 2 and Equation 3 respectively.

The Earth angle (γ_j) can be derived for each range sample as:

$$\gamma_j = a\sin\left[R_j\left(\sin(\alpha_j)\right)/R_{sat}\right] \qquad (2)$$

and the elevation angle θ_j is:

$$\theta_j = \alpha_j - \gamma_j \quad (3)$$

where j increases from 1 to N.

All the images were multi-looked in azimuth direction 10 times and the range direction 2 times to reduce the speckle noise. Later, the slant range was converted to ground range using ENVI software. The final spatial resolution of the data was about 20m x 20m with slight variation with incidence angle. Later, data were subjected to speckle filtering using Enhanced Lee filter [23]. Finally, backscattering coefficient was expressed in decibel units by taking 10Log10 (□0j). Only VV polarized images of April 23, 2006 and November 4, 2006 were considered for damage assessment analysis.

As we did not have topographic maps of the study area for geocoding SAR images, we took four corner coordinates provided in the metadata of Envisat ASAR product and geocoded the images. Later, image to image registration was done by identifying some Ground Control Points (GCPs) in both the images.The range of incidence angle (degree) for April 23, 2006 and November 4, 2006 of Envisat ASAR images was 30.8-36.177 and 30.84-36.15 respectively.

After preprocessing of Envisat ASAR images, all the values were obtained in dB i.e. backscattering values. Later on, these images were imported to ERDAS Imagine (version 9.3) for further analysis. The geographical areas of nine mandals of Guntur district were extracted from April 23, 2006 and November 4, 2006 Envisat ASAR images using a standard digitized vector layer.

2.2 METHODS

ANN is a machine learning technique that tries to mimic some of the processes of the human mind. It is highly interconnected set of simple computational units also called as nodes. These units roughly represent the biological neurons in the human brain. Like the brain, the synaptic weights in neural network learn by adapting the strength of the synaptic connections causing the neural network to 'learn'. Learning or training is a procedure that allows the network to adjust itself by means of gradually changing the network connection weights. Detailed mathematical description of multiple neural network models with their architecture and learning algorithms can be found in [24].

In this study, we used multilayer feed forward neural network model to identify the backscattering values of known water and non-water from the preprocessed data of Envisat ASAR images. For training, the data sets were divided randomly into training and test data sets. 70% of the data were used for building the model and called as training set. The remaining 30 % of the data (called as test set) were used to test the accuracy of the model [25]. Therefore, out of 406 pixels, 91 pixels of water and 315 pixels of non-water were used as the training data. Independent variables were standardized before training in the neural network model. To train the model, we used Levenberg-Marquadt algorithm [24].

The final architecture of the model contained one node in each if the three layers. Single node in the output layer was used as it was a binary classification problem. In the hidden layer, a single node was found to be enough though experiments were conducted with alternative architectures as well. The activation function was used at the hidden layer was *tanh* and at the output layer the logistic activation function was used. Weight decay parameter value of 0.5 was found to have better performance with the selected architecture.

The plot of the training data containing water and non-water pixels is shown in Figure 3. It shows that there was an overlap between backscattering values of water and non-water.

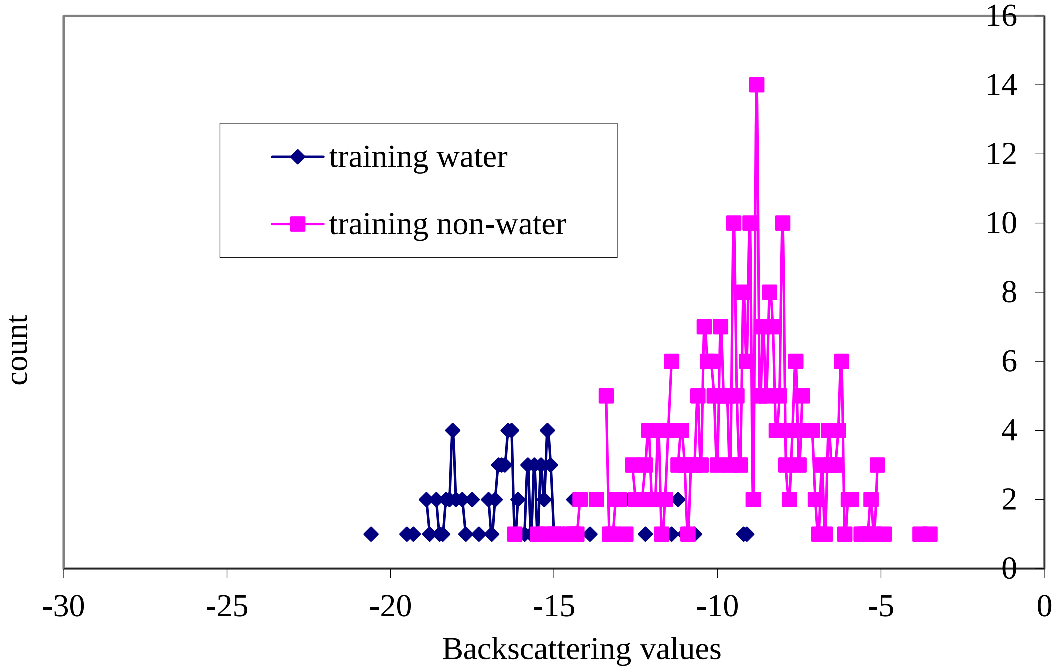

Figure 3 Plot of training water and non-water pixels backscattering values

The descriptive statistics of training water and non-water of Envisat ASAR image of April 23, 2006 is given in Table 1. The range of training water backscattering was from -20.6 dB to -9.1 dB, whereas, the range of training non-water backscattering values was from -16.2 dB to -3.5dB. If we selected -9.1 dB as the threshold, then, 163 pixels of non-water were classified as water whereas if -16.2 dB was selected as the threshold, then, 42 pixels of water were classified as non-water. The extreme selection of threshold led to overestimation or underestimation of either of the landcover class i.e. water or non-water. A threshold of -9.1 will lead to overestimation of water area and underestimation of non-water area. Similarly, selecting of threshold of -16.2 dB as the threshold, will led to underestimation of water area and over estimation of non-water area. A total of 205 pixels were placed in the common region (i.e. -16.2 to -10.7 dB).

Table 1: Descriptive statistics of training water and non-water pixels

Parameter/Class	Water	Non-water
Mean	-15.9	-9.3
Median	-16.3	-9.1
Mode	-18.2	-13.7
Standard Deviation	2.3	2.2
Kurtosis	0.9	0.2
Skewness	1.0	-0.3
Range	11.5	12.6
Minimum	-20.6	-16.2
Maximum	-9.1	-3.5
Count	91.0	315.0

The trained model was applied to test dataset to classify water and non-water. Confusion matrix for test dataset was generated and the overall accuracy was calculated for the Envisat ASAR image of April 23, 2006. The confusion matrix results of test data set are given in Table 2. The overall accuracy for the test set was 87.97%.

Table 2: Confusion matrix for test set of April 23, 2006

Known / Classified	Water	Non-water
Water	22	19
Non water	0	117

Overall accuracy=139/158=87.97%

Further, the trained model was applied to the complete image to get water and non-water areas in nine mandals of Envisat ASAR image of April 23, 2006. It was found that the total water area in the nine mandalsof Envisat ASAR image of April 23, 2006 was 2.344 thousand hectares. The trained model was applied to the post event Envisat ASAR image of November 4, 2006 to obtain completely submerged and partially/non submerged areas under water. The completely submerged land cover under water in nine mandals of Guntur district on November 4, 2006 was found to be 13.2705 thousand hectares. Further, using Press Q statistics for the test sample data showed that the accuracy predictions were significantly better than chance [26].

The spatial distribution of water in pre event image of April 23, 2006 and completely submerged areas under water in the post event Envisat ASAR image of November 4, 2006 are shown in Figure 4 and Figure 5 respectively.

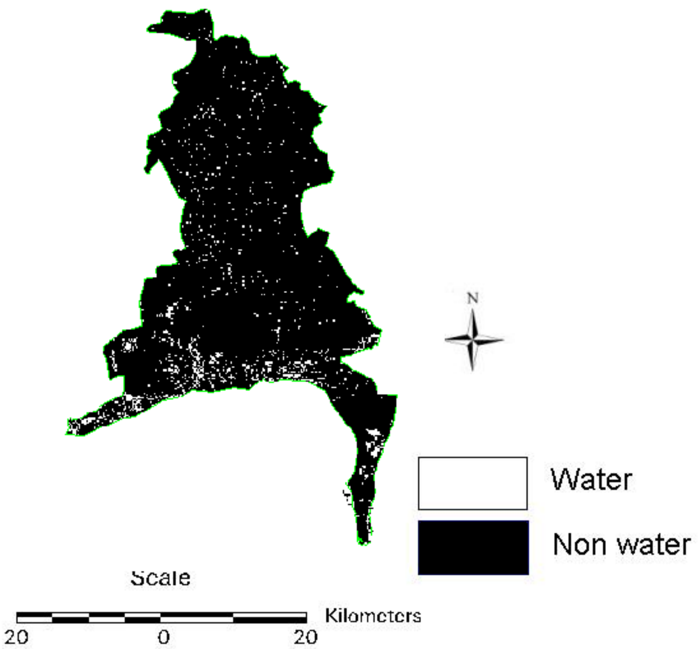

Figure 4 Spatial distribution of water in Envisat ASAR image of April 23, 2006

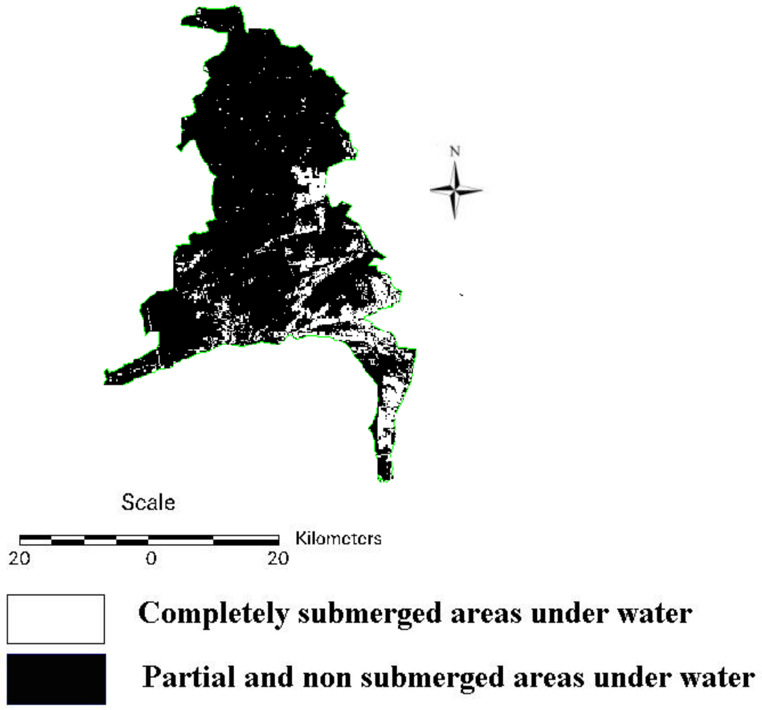

Figure 5 Spatial distribution of completely submerged area in Envisat ASAR image of November 4, 2006

5.0 CONCLUSION, LIMITATION AND FUTURE WORK

The flooded area extraction was attempted using Envisat ASAR VV polarized data by ANN. This technique reduced the overestimation or underestimation of water and flooded areas and the results were comparable with other techniques [27]. In the present study, the water and non-water training pixels were very small compared to the total pixels of the study area. The application of this method at district/sub-district level for the flood studies would require development of infrastructure facilities at the grass root level. In future work, we will apply this method to other SAR data

ACKNOWLEDGEMENTS

The research was funded by National Science Foundation, USA through Nodal Agency CMU, USA under the theme of Integrated Assessment of Human Dimensions of Global Change.

REFERENCES

[1] Abhyankar, A. A., Singh, A., Sharma, U., Patwardhan, A. and Inamdar, A. (2004). Constructing a tropical cyclone hazard index for coastal India, International Symposium on Natural Hazards, Hyderabad, February 24-28.

[2] Hess, L. L., Melack, J. M., Filoso S. and Wang, Y. (1995). Delineation of Inundated Area and Vegetation along the Amazon Floodplain with the SIR-C Synthetic Aperture Radar. IEEE Transactions of Geoscience and Remote Sensing, 33 (4), 896-904.

[3] Toan, T. L, Ribbes, F., Wang, L., Floury, N. and Ding, K. (1997). Rice crop mapping and monitoring using ERS-1 data based on experiment and modeling results. IEEE Transactions of Geoscience and Remote Sensing, 35(1), 41-55.

[4] Ormbsy, J. P., Blanchard, J. P. and Blanchard, A. J. (1985). Detection of lowland flooding using active microwave systems, Photogrammetric Engineering and Remote Sensing, 51, 317-328.

[5] Ribbes, F. and Toan, T. L. (1998). Mapping and Monitoring Rice crop with Radarsat Data, Geoscience and Remote Sensing Symposium, IGARSS '1998 Proceedings, IEEE International, 2749-2751.

[6] Imhoff, M. L., Verimillion, C., Story, M., Choudhury, A. and Gafoor, A. (1987). Monsoon flood boundary delineation and damage assessment using space borne imaging radar and Landsat data, Photogrammetric Engineering and Remote Sensing, 53, 405-413.

[7] Schumann, G., Hostache, R., Puech, C., Hoffmann, L., Matgen, P., Pappenberger, F. and Pfister, L. (2007). High-resolution 3-D flood information from Radar imagery for flood hazard management, IEEE Transactions on Geoscience and Remote Sensing, 45(6), 1715-1725.

[8] Chokmani, K., Bernier, M., Poulin, J. and Raymond S. (2017). River flood mapping in urban areas combining Radarsat-2 data and flood return period data, Remote Sensing of Environment, 198(1), 442-459

[9] Jiren, L. and Shifeng, H. (2005). Application of ERS/ENVISAT to flood monitoring and assessment in China, IEEE International Geoscience and Remote Sensing Symposium, 8, 5674-5677.

[10] Ramsey III, E., Rangoonwala, A. and Bannister, T. (2013). Coastal flood inundation monitoring with satellite C-band and L-band synthetic aperture radar data, Journal of the American Water Resources Association, 49(6), 1239-1260.

[11] Yamada, Y., Sakurai-Amano, T. and Takagi, M. (2002). Detection of flood damaged areas in the entire Chao Phraya River Basin from JERS-1/SAR images with a help of spatial information, IEEE International Geoscience and Remote Sensing Symposium, 5, 2877-2879.

[12] Badji, M. and Dautrebande, S. (1997). Characterization of flood inundated areas and delineation of poor drainage soil using ERS-1 SAR imagery, Hydrological Processes, 11(10), 1441-1450.

[13] Shao, Y., Fan, X., Liu, H., Xiao, J., Ross, S., Brisco, B., Brown, R. and Saples, G. (2001). Rice Monitoring and production estimation using multi-temporal Radarsat, Remote Sensing of Environment, 76, 310-325.

[14] Lee, K. S. and Lee, S. I. (2003). Assessment of post-flooding conditions of rice fields with multi-temporal SAR data. International Journal of Remote Sensing, 24 (17), 3457-3465.

[15] Henry, J. B., Chastanet, P., Fellah, K. and Desnos, Y.L. (2003). Envisat multi-polarized ASAR data for flood mapping, IEEE International Geoscience and Remote Sensing Symposium, 2, 1136-1138.

[16] Yang, C., Huang, H., Wei, Y., Zhu, H. and Zhuo, J. (2002). Rapidly Assessing the flood Disaster by using Remote sensing and GIS, Geoscience and Remote Sensing Symposium, IGARSS '02, IEEE International, 5, 2880-2882.

[17] Malnes, E., Guneriussen, T. and Hogda, K. A. (2002). Mapping of flood area by Radarsat in Vansjo, Norway http://projects.itek.norut.no/snowman/Publications/Malnes1_ISRSE_2002.pdf (last accessed on July 31, 2013).

[18] Abhyankar, A. A., Patwardhan, A. and Inamdar, A. B. (2012). Estimation of Flooded Areas due to Supercyclone using Radarsat-1 SAR Data and Discriminant Approach-An Indian Case Study, paper presented at the 33rd Asian Conference on Remote Sensing, Pattaya, Thailand, November 26-30.

[19] Notes on Cyclone Damages and Relief Measures, Guntur district {Submitted to Inter Ministerial Team (09-11-2006 and 10-11-2006); Collector and District Magistrate, Guntur; unpublished (2006)}.

[20] Agriculture Production Plan, Agriculture Department, Guntur District, 2008-2009.

[21] Director of Economics and Statistics, 2006, Government of India, Andhra Pradesh, Hyderabad

[22] Rosich, B. and Meadows, P. (2004). Absolute Calibration of ASAR Level 1 Products Generated with PF-ASAR, ENVICLVL-EOPG-TN-03-0010, Issue 1, date of issue: October 7, 2004, revision 5, Technical note http://earth.esa.int/pub/ESA_DOC/ENVISAT/ASAR/ASAR_products_absolute_calibration_v1.5.pdf (last accessed on September 15, 2009).

[23] Zhenghao, S. and Fung, K. B. (1994). A Comparison of Digital Speckle Filters, IEEE International Geoscience and Remote Sensing Symposium, 4, 2129-2133.

[24] Haykins, S. (2005). Neural Networks: A Comprehensive Foundation, Second Edition, Pearson Prentice Hall.

[25] Paliwal, M. and Kumar, A. K. (2009). Neural Network and Statistical Techniques: A Review of Applications. Expert Systems with Application, 36, 2-17.

[26] Hair, J., Anderson, R., Tatham, R. and Black, W. (1998). Multivariate Data Analysis, Fifth edition, Prentice-Hall.

[27] Abhyankar, A. A. (2010). Rapid Assessment of Tropical Cyclone Impacts Using Remote Sensing with Application to Disaster Management, PhD. Thesis, IIT Bombay (unpublished).